

Caloric curves for small systems in the nuclear lattice gas model

C. B. Das and S. Das Gupta

Physics Department, McGill University, 3600 University Street, Montréal, Québec, Canada H3A 2T8

(Received 26 September 2000; published 31 May 2001)

For pedagogical reasons we compute the caloric curve for 11 particles in a 3^3 lattice. Monte Carlo simulation can be avoided and exact results are obtained. We compare canonical and microcanonical results for the caloric curve. Even down to this small system, agreement between the canonical model and the microcanonical model is surprisingly good. We point out that the introduction of kinetic energy in the nuclear lattice gas model modifies the results of the standard lattice gas model in a profound way. The model is also used to test the accuracy of the saddle-point approximation for density of states.

DOI: 10.1103/PhysRevC.64.017601

PACS number(s): 25.70.Pq, 24.10.Pa, 64.60.My

In a recent paper [1], we pointed out that microcanonical calculations in the lattice gas model (LGM) with constant energy are no harder to implement than canonical calculations with constant temperature. We will call the first MLGM, and the second, CLGM. For practical cases at hand ($A \approx 100$ or 200), the calculations use Monte Carlo simulations with Metropolis algorithm.

In this Brief Report we take a small system and do LGM calculations without any Monte Carlo simulation. The reasons for doing these “exact” calculations are the following: (1) we see if there are substantial differences between microcanonical and canonical results for such small systems, (2) if anomalies in caloric curves arise because of extreme finiteness, and (3) this constitutes an example where an exact density of states can be compared with an approximate density of state obtained from the saddle-point approximation. The latter is of course of frequent use in nuclear physics [2] and this is a case where, unlike many other cases, numerical accuracy can be easily verified.

In our example, we take 11 particles in a 3^3 cubic lattice. As our objective is solely pedagogical, we assume there is just one kind of particles (nucleons). We have then a freeze-out density $0.41\rho_0$ which is somewhat higher than the freeze-out density used in lattice gas model calculations [3]. The nearest neighbor bonds are attractive: $\epsilon = -5.33$ MeV to get the nuclear matter binding energy correct.

The nuclear lattice gas model which is denoted here by LGM is an extension of the standard textbook lattice gas model as discussed, for example, in [4]. We denote the standard lattice gas model by SLGM. The difference is simple: in SLGM, the nucleons are frozen in their lattice sites. In LGM, dictated by the physics of the nuclear problem, they are given momenta. In CLGM, these momenta are generated using a Maxwell-Boltzmann distribution. In MLGM, they are taken from a uniform distribution within a sphere in momentum space. The addition of kinetic energy, however, changes the caloric curve in an interesting and profound way. We will find it useful to discuss the caloric curves in both SLGM and LGM. Chronologically, it is easier to discuss SLGM first, then point out how LGM modifies the results. In both the models the key quantities are $G(27, 11, N_{nn}) \equiv g(N_{nn}) =$ the number of configurations with N_{nn} nearest neighbor bonds for the case of 11 particles in 3^3 lattice sites. Once these are known both canonical and microcanonical calculations are

readily done. The degeneracy factors are given in Table I. They can be obtained with little effort in this simple case.

Instead of writing $g(N_{nn})$ we will find it convenient to write g as a function of E^* where E^* is the excitation energy. The degeneracy factor $g(E^*)$ as a function of $E^*/|\epsilon|$ is plotted in Fig. 1. The distribution is discrete but in Fig. 1 we show it as a continuous distribution and label the y axis by $dN(E^*)/d|\epsilon|$. If one wants to define a temperature, the standard practice in the microcanonical model is to compute $\partial \ln \Omega(E^*)/\partial(E^*) \equiv 1/T$ (see [5]). An inspection of Fig. 1 shows that as a function of excitation energy the temperature will rise first, approach $+\infty$, will then switch towards $-\infty$ and as the excitation energy will further increase the temperature will approach 0 from the negative side. This happens because in SLGM there is an upper bound to energy. This is of course well known for spin 1/2 systems in a magnetic field if the kinetic energy of the spin system is suppressed [5].

The caloric curve in microcanonical SLGM is shown in

TABLE I. Degeneracy factors $g(N_{nn})$ with N_{nn} nearest neighbor bonds.

N_{nn}	$g(N_{nn})$
0	462
1	888
2	8511
3	38 128
4	150 030
5	481 368
6	1 171 492
7	2 106 504
8	2 772 894
9	2 643 624
10	1 895 907
11	1 051 632
12	481 610
13	174 408
14	50 301
15	8984
16	1056
17	96

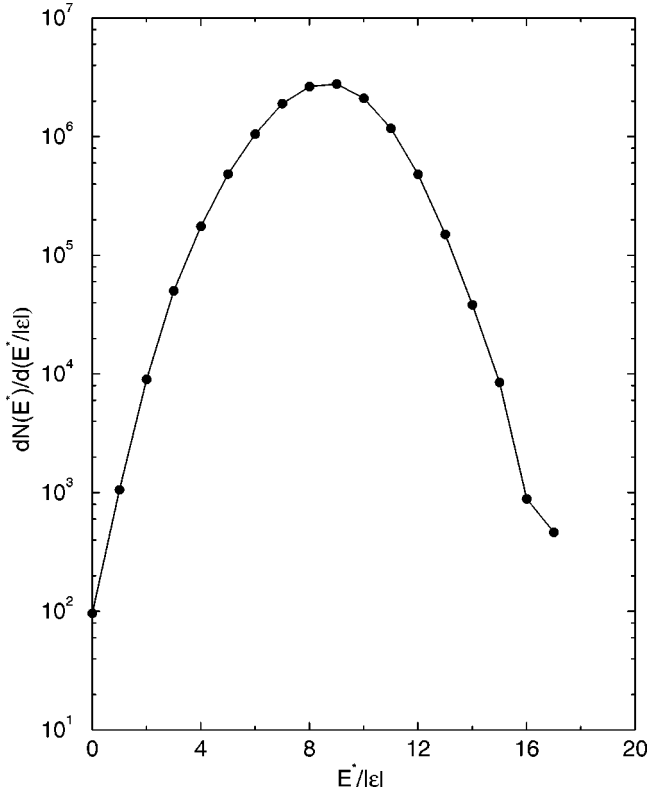


FIG. 1. The density of states in the standard lattice gas model. This can be directly obtained from the table remembering that $N_{nn}=17$ defines the ground state.

Fig. 2. In plotting this curve we used degeneracies of successive discrete points in the excitation energy and divided by $|\epsilon|$ to get the temperature. Notice that in the positive side of the temperature there is no anomalous behavior. If we plot E^* along the y axis and T along the x axis, the temperature will suddenly flip to large negative value at about half the excitation energy available to the system. But this is merely a reflection of the fact that the excitation energy available to the system is finite. This will drastically change in the nuclear LGM where availability of kinetic energy will remove the upper limit.

For canonical calculation, we pick a positive temperature: to get the caloric curve we compute $\langle E \rangle = \sum \epsilon N_{nn} \times g(N_{nn}) \exp(-\beta N_{nn} \epsilon) / \sum g(N_{nn}) \exp(-\beta N_{nn} \epsilon)$. Subtracting out the ground state energy we obtain the plot in Fig. 2. The same procedure can be used for negative temperature. Both are used in Fig. 2. The similarity between caloric curves calculated in the microcanonical and canonical models is obvious although there are quantitative differences.

From SLGM we now turn to nuclear LGM which serves as a model for nuclear disassembly. This was the case presented in [1]. The excitation energy can come from two sources now: kinetic and potential. Consequently, we compute $\sum_i g(E_i^*) \rho_{kin}(E^* - E_i^*)$ where $g(E_i^*)$ is discrete and taken from the table and $\rho_{kin}(E_{kin})$ is taken to be the integral

$$\int \delta\left(E_{kin} - \sum p_i^2/2m\right) \Pi d^3 p_i = \frac{(\sqrt{\pi})^{3N}}{\Gamma(3N/2)} (2m)^{3N/2} E^{3N/2-1}. \quad (1)$$

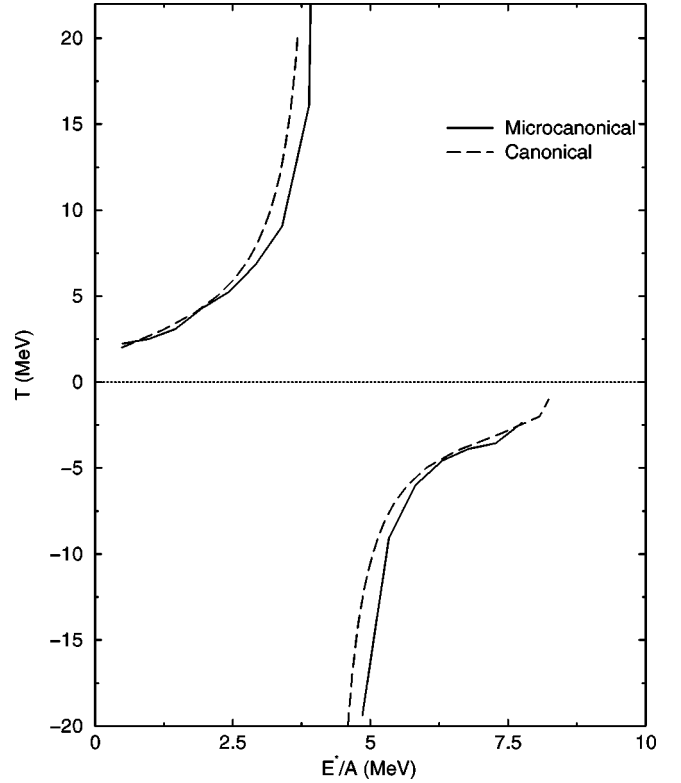


FIG. 2. The caloric curve in SLGM. From Fig. 1 it is clear that the microcanonical definition of temperature would tend to infinity around $E^*/|\epsilon| \approx 8$. For 11 particles this corresponds to about 4 MeV excitation per particle. At higher excitations, the standard definition of temperature leads to large negative temperature. In the canonical calculation, we assume a temperature (positive and negative) and obtain $\langle E^*/A \rangle$ using the table.

N in our chosen case is 11. Now there is no upper limit to E^* . In Fig. 3 we have plotted $\sum_i g(E_i^*) \rho_{kin}(E^* - E_i^*)$. The most important difference from Fig. 1 is that the negative temperature zone has completely disappeared. Thus the difference in the caloric curves obtained from SLGM and LGM will be profound.

There are two ways one can calculate the temperature in the microcanonical model. One is the standard formula: $1/T = \partial \ln \Omega(E^*) / \partial E^*$, where

$$\Omega(E^*) \propto \sum_i g(E_i^*) \rho_{kin}(E^* - E_i^*). \quad (2)$$

The other intuitive approach would be to make the following ansatz. Although we are talking of one system only, formally Eq. (2) is similar to that of two systems characterized by g and ρ_{kin} which share energy with each other but are insulated from the rest of the universe so that the total energy E^* does not change. If the systems characterized by g and ρ are large then the sum above would be dominated by the largest term in the sum which is obtained when the temperature of each subsystem is the same, i.e., $\partial \ln g(E_i^*) / \partial E_i^* = \partial \ln \rho_{kin}(E_{kin}) / \partial E_{kin}$. We now use $1/T = \partial \ln \rho_{kin}(E_{kin}) / \partial E_{kin}$. This leads to $\langle T \rangle = \langle E_{kin} \rangle / (1.5N - 1)$. This $\langle T \rangle$ and the stan-

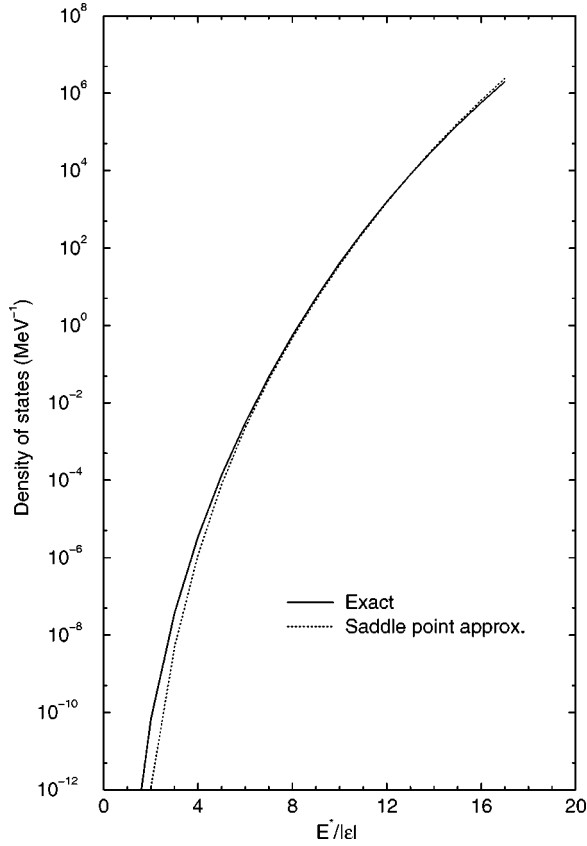


FIG. 3. The density of states in the nuclear LGM. We have plotted (the solid curve) $\sum_i g(E_i^*) \rho_{kin}(E^* - E_i^*)$. For ρ_{kin} we have used Eq. (1) and multiplied it by $(V/h^3)^N$ where $V = 27/0.16 \text{ fm}^3$. The dotted curve is the saddle-point approximation for the same density of states. Here $Q(\beta_0)$ is separable into two parts. One part comes from the potential and is directly calculable from the table. This is multiplied by $(2\pi mT)^{3N/2}$ which comes from the kinetic energy.

standard definition of T agree quite well as can be seen in Fig. 4. Notice also there is no backbending in the microcanonical caloric curve. If one wants to use the microcanonical nuclear LGM for practical calculations with nucleon numbers about 100 or higher and also wants to obtain a value for temperature, getting the temperature from kinetic energy is the only easy option.

In Fig. 4 we have also shown the caloric curve in nuclear LGM in the canonical model. This agrees with the microcanonical calculation quite well.

In the particular example (11 particles in 3^3 boxes in the nuclear LGM), one has exact expressions for microcanonical density of states. One can also compute numerically the canonical partition function. In nuclear physics one often has numerical values for canonical or grand canonical partition functions. The direct expression for the microcanonical density of state is usually intractable and in order to obtain a value one uses the saddle-point approximation [2,6]. We can use the nuclear LGM to test the accuracy of the saddle-point approximation since here both the microcanonical density of state and the canonical partition function are directly calculable. The microcanonical density of states and the canonical

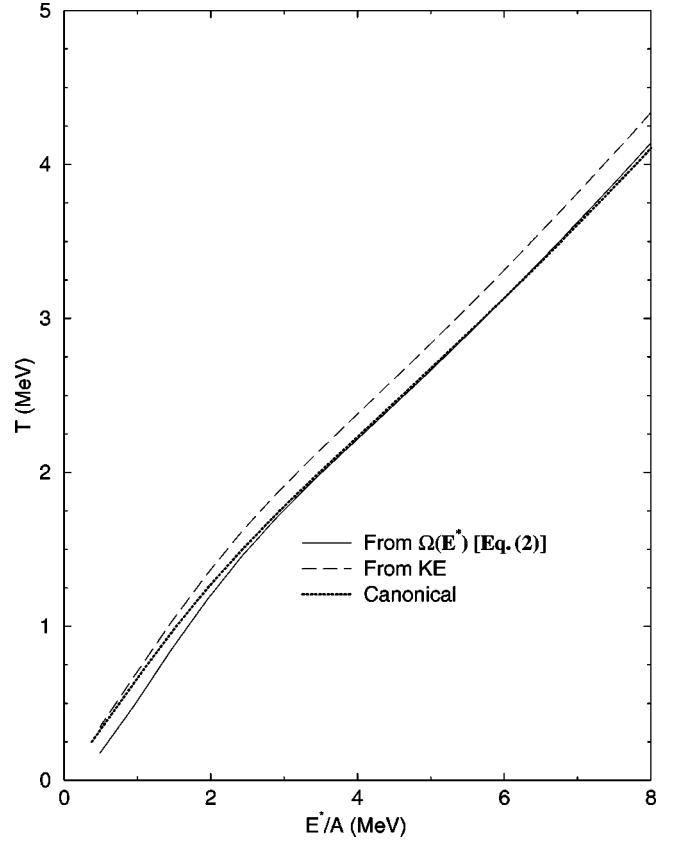


FIG. 4. The caloric curve in microcanonical and canonical treatments. For microcanonical we show two curves. The solid curve takes the log of Eq. (2) and differentiates with respect to E^* to obtain a temperature. The dashed curve defines T from the average value of kinetic energy (see text). The dotted curve is the canonical caloric curve for the nuclear LGM.

partition function are related by $Q(\beta) = \int \exp(-\beta E) \rho(E) dE$. The inverse transformation is

$$\rho(E) = \exp(\beta_0 E) (1/2\pi) \int \exp(i\beta E) Q(\beta_0 + i\beta) d\beta.$$

The saddle-point approximation for this integral leads to

$$\rho(E) \approx \frac{\exp[\beta_0 E + \ln Q(\beta_0)]}{\sqrt{2\pi(\langle E^2 \rangle - \langle E \rangle^2)}}, \quad (3)$$

where the value of β_0 is so chosen that at this value $\langle E \rangle = E$. The saddle-point approximation for the density of states is also compared to the exact density of state in Fig. 3. Except for low excitation energies, the saddle-point approximation is seen to be excellent.

For the case of 11 particles in a 3^3 lattice we have done exact microcanonical and canonical calculations for the caloric curve. The main result of this Brief Report is that even for this small number of particles there is surprising agreement between the two models. This is true even though we are far from the thermodynamic limit. In the models considered no anomalous behavior in caloric curve is found.

After this paper was submitted, a different formulation of the LGM was published [7] where a negative specific heat

was found. In this last model volume is not a constant as in our calculation (and most LGM calculations) but an average volume was fixed by use of a Lagrange multiplier which weighted each configuration with $\exp(-\lambda V)$ where V is the “volume” of the configuration. Negative heat capacities have also been discussed in other contexts [8–10].

Lastly, the saddle-point approximation for density of

states was compared with an exact density of states. Agreement was found to be very good.

This work was supported in part by the Natural Sciences and Engineering Council of Canada and by *le Fonds pour la Formation de Chercheurs et l'Aide à la Recherche du Québec*. We acknowledge communications with Professor Dieter Gross.

-
- [1] C.B. Das, S. Das Gupta, and S.K. Samaddar, *Phys. Rev. C* **63**, 011602(R) (2001).
- [2] A. Bohr and B.R. Mottelson, *Nuclear Structure* (Benjamin, New York, 1969), p. 281.
- [3] J. Pan and S. Das Gupta, *Phys. Rev. C* **51**, 1384 (1995).
- [4] K. Huang, *Statistical Mechanics* (Wiley, New York, 1987), Chap. 14.
- [5] F. Reif, *Fundamentals of Statistical and Thermal Physics* (McGraw-Hill, New York, 1965), Chap. 3.
- [6] P. Bhattacharyya, S. Das Gupta, and A.Z. Mekjian, *Phys. Rev. C* **60**, 064625 (1999).
- [7] P. Chomaz, V. Duflo, and F. Gulminelli, *Phys. Rev. Lett.* **85**, 3587 (2000).
- [8] J.M. Carmona, N. Michel, J. Richert, and P. Wagner, *Phys. Rev. C* **61**, 037304 (2000).
- [9] D.H.E. Gross and E.V. Votyakov, *Eur. Phys. J. B* **15**, 115 (2000).
- [10] L.G. Moretto, J.B. Elliott, L. Phair, and G.J. Wozniak, *nucl-th/0012037*.